JOURNAL OF Applied Polymer SCIENCE

Two Courses in the Nonisothermal Primary Crystallization of Poly(butylene terephthalate)

Xi Wang, Xingyuan Zhang, Long Zhang
CAS Key Laboratory of Soft Matter Chemistry, Department of Polymer Science and Engineering, University of Science and Technology of China, Hefei, Anhui 230026, People's Republic of China
Correspondence to: X. Zhang (E-mail: zxym@ustc.edu.cn)

ABSTRACT: Nonisothermal crystallization behavior of poly(butylene terephthalate) (PBT) was investigated by means of differential scanning calorimetry. The nonisothermal crystallization kinetic process was analyzed and relative kinetic parameters were obtained with the Avrami and Liu–Mo equations. The results demonstrate a heterogeneous nucleation mechanism. It was found that the nonisothermal primary crystallization of PBT was composed of two courses. Course I corresponded to the two-dimensional formation process of the lamellae, and the corresponding relative crystallinity (X_t) was less than 15%. Course II was concerned with the three-dimensional growth process of the spherulite, and X_t changed from 15 to 90%. The secondary crystallization began when X_t was greater than 90%. According to the Flynn–Wall–Ozawa equation, the activation energies for course I, course II, and secondary crystallization were calculated to be −120, −210, and −100 kJ/mol, respectively. © 2012 Wiley Periodicals, Inc. J. Appl. Polym. Sci. 000: 000–000, 2012

KEYWORDS: poly(butylene terephthalate); nonisothermal crystallization; primary crystallization; two courses

Received 4 November 2010; accepted 4 June 2012; published online
DOI: 10.1002/app.38160

INTRODUCTION

Poly(butylene terephthalate) (PBT) is a semicrystalline thermoplastic polymer with a rapid crystallization rate, and it is well suited for injection molding because of its low mold shrinkage, excellent dimensional stability, high mechanical strength, and good solvent resistance. The physical and mechanical properties of the product are directly related to the microstructure, which is determined by the extent of crystallization and influenced by the nonisothermal conditions set forth during practical processing. Therefore, the nonisothermal crystallization kinetics can be used to clarify the crystallization behavior and provide a theoretical basis for the formation of crystals.

PBT can form α crystals by nonisothermal crystallization.[1–3] For the nonisothermal crystallization of PBT, the investigation of crystallization kinetics has mainly focused on differential scanning calorimetry (DSC); however, the observation of crystalline morphology has been carried out with the methods of small-angle laser scattering, time-resolved X-ray diffraction, and transmission electronic microscopy.[4–10] Although Ozawa, Ziabicki, Jeziorny, Gupta, Liu, and some other models could be used to analyze and discuss the nonisothermal crystallization process, most of them were unable to accurately describe the entire process because nonisothermal crystallization kinetics are more complex than isothermal kinetics.[11–16] Until recently, most researchers have analyzed and processed the kinetic data with a $\log \Phi \sim \log t$ (where t is the crystallization time and Φ is the cooling rate) linear relationship and demonstrated a nonisothermal crystallization mechanism based on the related kinetic parameters. By analyzing the primary crystallization kinetic parameters of the nonisothermal crystallization of PBT, Huang[17] and Yao et al.[18] suggested a mechanism of thermal nucleation and three-dimensional spherical growth, Al-Mulla et al.[19] considered a model of heterogeneous nucleation and three-dimensional growth, and Bai et al.[20], Kalkar and Deshpande,[21] and Wu et al.[22] provided some mechanisms, including three-dimensional morphological growth preceded by instantaneous nucleation, instantaneous nucleation with diffusion control, and a reflection of memory effects.

Combining the Avrami and Ozawa equations, Liu, Mo, and coworkers[15,16] proposed a novel method to exactly describe the nonisothermal crystallization process. The Liu–Mo method can solve the problems of fewer data points, the often appearing nonlinear relationship, and the difficulty in getting reliable kinetic parameters with the Ozawa equation. The method is also able to overcome the shortcoming that the mechanism of nucleation and growth during nonisothermal crystallization cannot be predicted accurately on the basis of the apparent Avrami exponent (n) obtained from the Avrami equation modified by Jeziorny.

Applied Polymer SCIENCE

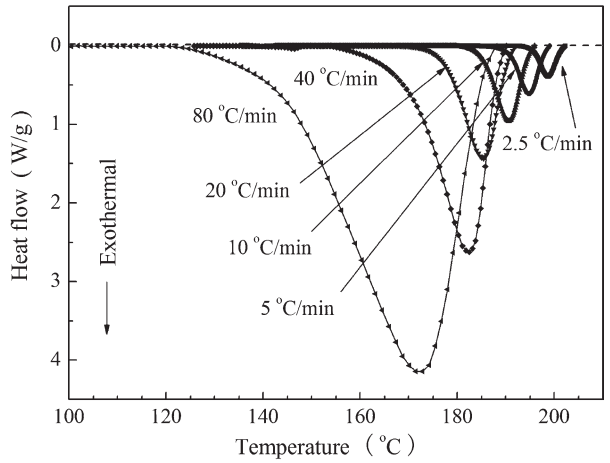

Figure 1. Heat flow versus temperature during the nonisothermal melt crystallization of PBT at different Φ's.

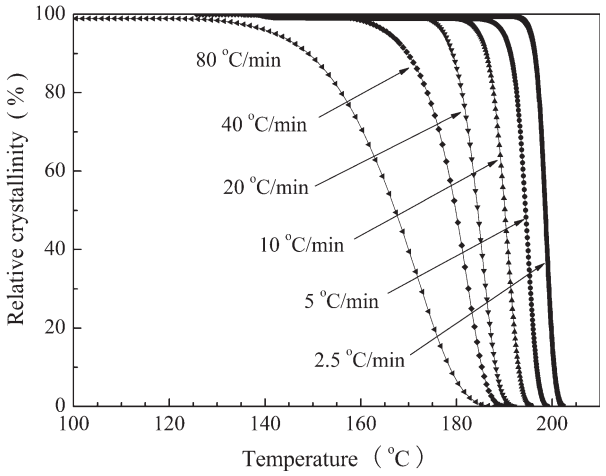

Figure 2. X_t versus temperature during the nonisothermal melt crystallization of PBT at different Φ's.

In this study, the nonisothermal crystallization behavior of PBT was investigated by means of DSC. The nonisothermal crystallization process could be regarded as the superposition and combination of numerous successive micro-isothermal processes; this means that the nonisothermal crystallization kinetics can be analyzed by the Avrami equation. By applying the Avrami equation and the Liu–Mo method to analyze and discuss the kinetic parameters, we discovered that not only could the Liu–Mo method entirely characterize the nonisothermal crystallization process of PBT, including the primary and secondary crystallization, but also the nonisothermal primary crystallization of PBT could be divided into two courses, the two-dimensional formation of lamellar crystals and the three-dimensional growth of spherulites. Furthermore, the activation energy (E_a) of nonisothermal crystallization was evaluated with the Kissinger and Flynn–Wall–Ozawa (FWO) methods.

EXPERIMENTAL

PBT (weight-average molecular weight = 83,000) was provided by the Chang Chun Plastics Co., LTD (Taiwan, China) under the trade name PBT-1100 and had a density of 1.3 g/cm^3 and a melt index of 18–22 g/10 min (ASTM D 1238). PBT pellets were dried at 100°C in a vacuum oven for 6 h before the test. A Mettler–Toledo DSC1 differential scanning calorimeter (Zurich, Switzerland) was used to perform the nonisothermal crystallization experiments. The calibration was done with standard indium and zinc sealed in aluminum pans. All operations were carried out in a high-purity nitrogen atmosphere. For cooling experiments, each sample prepared from the pellets was heated to 260°C for 10 min to ensure the elimination of the thermal history, and the complete melting of the PBT sample was achieved. Then, the sample was cooled down at various Φ's (2.5, 5, 10, 20, 40, and 80°C/min) to 40°C. The exothermal nonisothermal crystallization curves of the heat flow as a function of time were recorded using the software provided by Mettler–Toledo.

RESULTS AND DISCUSSION

Nonisothermal Primary Crystallization Kinetic Analysis by the Avrami Equation

Figure 1 shows the nonisothermal crystallization DSC curves of PBT at different Φ's after the baseline is subtracted. The exothermic peak of PBT crystallization at each Φ was mainly a single peak. With increasing Φ, the exothermic peaks gradually shifted to lower temperatures, and the shapes of the peaks also widened.

By comparing the onset temperature (T_0) and end temperature of the nonisothermal crystallization temperature of the exothermic peaks at different Φ's, we found that both temperatures decreased with increasing Φ. In addition, the temperature at the end of crystallization of the exothermic peaks decreased even more steeply. Generally, the crystallization T_0 is higher with a lower Φ; this indicates that the system has enough time to cross the nucleation barrier. Alternatively, at a higher Φ, T_0 is lower; this reflects a higher nucleation efficiency at lower temperatures.[23]

The relative crystallinity (X_t) as a function of temperature was calculated as the ratio of the exothermic peak areas in Figure 1 according to the definition of X_t. The curves of X_t versus temperature at different Φ's were inverse sigmoidal curves. The temperature abscissa in Figure 2 could be transformed into a timescale, as shown in Figure 3, on the basis of the following equation:

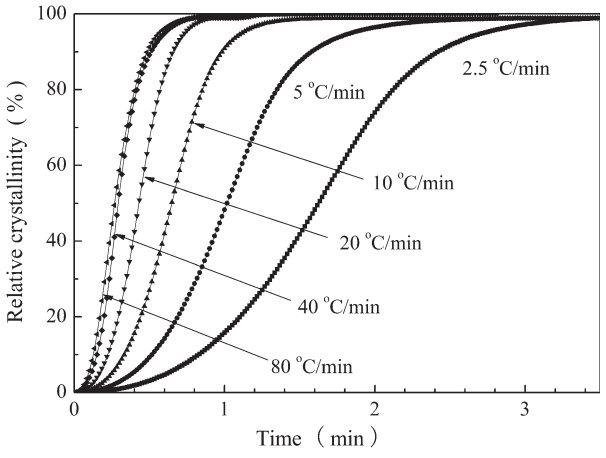

Figure 3. X_t versus time during the nonisothermal melt crystallization of PBT at different Φ's.

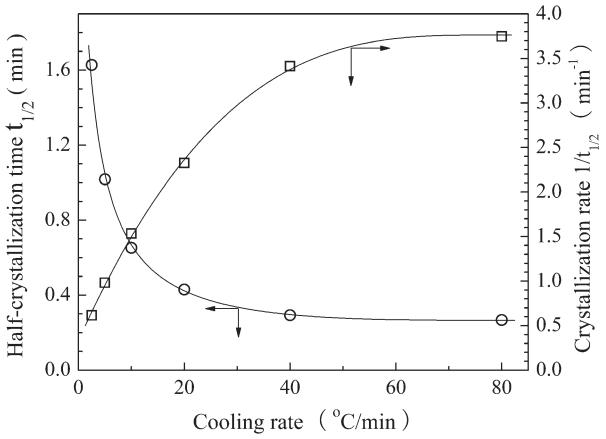

Figure 4. Relationships among $t_{1/2}$, crystallization rate, and Φ for the nonisothermal crystallization of PBT.

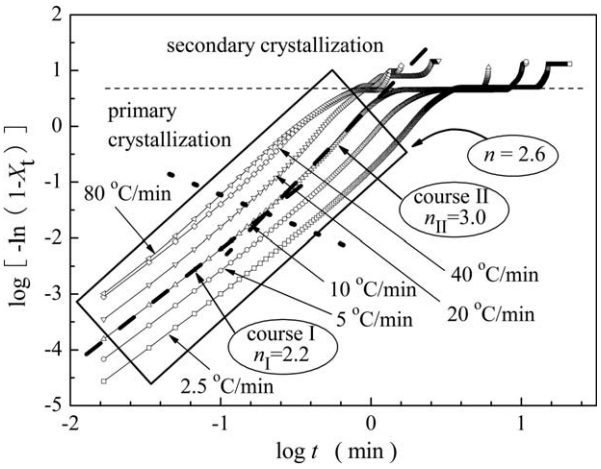

Figure 5. log[−ln(1 − X_t)] versus log t for the nonisothermal crystallization of PBT.

$$t = |(T_0 - T)/\Phi| \quad (1)$$

where T_0 and T are defined as the onset temperature when the crystallization started ($t = 0$) and the temperature at time t, respectively. It can be seen clearly from Figure 3 that the higher Φ was, the shorter the time was for completing the crystallization.

In general, for polymer crystallization, the half-crystallization time ($t_{1/2}$) is an important parameter. The inverse value of $t_{1/2}$ signifies the crystallization rate, and a higher $1/t_{1/2}$ value indicates faster crystallization. $t_{1/2}$ and crystallization rate ($1/t_{1/2}$) were obtained from Figure 3. The relationship between $t_{1/2}$ and the crystallization rate versus various Φ's are shown in Figure 4. When Φ was in the range 2.5–20°C/min, $t_{1/2}$ decreased rapidly with increasing Φ. Then, the rate of decrease leveled off. Moreover, the crystallization exothermic peak temperature (T_p) with different Φ's shared the same trend with $t_{1/2}$. The crystallization rate increased with increasing Φ; this indicated that PBT crystallized faster when Φ was higher.

The Avrami equation is often used to describe the nonisothermal crystallization of polymers. The Avrami equation is expressed as follows:

$$\log[-\ln(1 - X_t)] = \log k + n \log t \quad (2)$$

where k is the Avrami crystallization rate constant and n is the Avrami exponent, which indicates the crystallization mechanism.

The plot of log[−ln(1 − X_t)] versus log t for nonisothermal crystallization of PBT is shown in Figure 5. The entire crystallization process could be divided into two stages, that is, primary crystallization and secondary crystallization. In general, the primary crystallization data showed a cursory linearity on the basis of the Avrami equation analysis model. An average value of $n = 2.6$ was obtained at different Φ's; this was consistent with the results obtained and reported by Gilbert and Hybart[24] and Marrs et al.[25] Righetti and Munari[26] confirmed the theoretical spherulites of the crystalline morphology of PBT by optical microscopy; therefore, $n = 3$ for PBT. They, thus, pointed out the crystallization of PBT could be considered a heterogeneous nucleation with a three-dimensional crystal growth mechanism. As nonisothermal crystallization processes are more complex than the isothermal ones, the kinetic parameters significantly deviated from one straight line when the Avrami equation was simply used to analyze the nonisothermal crystallizations.

In fact, as shown in Figure 5, the primary crystallization of the nonisothermal crystallization was not one straight line. When the primary crystallization process was divided into two courses, courses I and II, noted in Figure 5, the experimental results indicate that for each process, log[−ln(1 − X_t)] and log t were in a linear relationship. To provide more analysis information for the two segments in Figure 5, Table I summarizes the fitting ranges of each linear fit, as shown later.

Table I. Fitting Ranges of log[−ln(1 − X_t)] and Its Slope (n) from Figure 5

Φ (°C/min)	log[−ln(1 − X_t)]	n	log[−ln(1 − X_t)]	n_I	log[−ln(1 − X_t)]	n_{II}
2.5	−4.6-0.3	2.6	−4.6-−1.2	2.2	−1.2-0.3	3.0
5	−4.2-0.3	2.6	−4.2-−1.2	2.2	−1.2-0.3	3.0
10	−3.8-0.3	2.6	−3.8-−1.1	2.2	−1.1-0.3	3.0
20	−3.4-0.3	2.6	−3.4-−1.1	2.2	−1.1-0.3	3.0
40	−3.1-0.3	2.6	−3.1-−1.0	2.2	−1.0-0.3	3.0
80	−3.0-0.3	2.6	−3.0-−0.9	2.2	−0.9-0.3	3.0

Applied Polymer SCIENCE

The detailed fitting quality parameters (r^2's) of the whole linear fit could not be calculated because of the distribution of the kinetic data points in Figure 5. Table I describes the fitting ranges of $\log[-\ln(1 - X_t)]$ of the two segments and the transition points of each two courses. It can be seen clearly that in the specific fitting ranges based on the Avrami equation analysis model, the primary crystallization data showed two straight lines. The transition between courses I and II might have been a gradual change because of the continuous crystallization process. However, on the basis of the linearity of the two segments also, there were not too many intermediate points in the transition region between two lines, as shown in Figure 5; the primary crystallization process could be divided mainly into two courses.

With the same Avrami equation, the slope of the fitted line for course I at different Φ's gave an Avrami exponent (n_I) of 2.2 and the Avrami exponent of course II (n_{II}) was 3.0. The arithmetic average value of n_I and n_{II} was 2.6, which agreed well with a rough Avrami equation treatment by one linear process. The n_I and n_{II} values were quite close to the integers 2 and 3, respectively. Therefore, the two n values of the primary crystallization process had clear physical meanings. That is, as course I was the initial stage of crystal growth, n_I, which was close to the integer 2, showed the initial stage of crystal growth and was the result of, first, the formation of nucleation and, then, two-dimensional crystal growth. After a period of crystal growth, course II took place and indicated a mechanism of heterogeneous nucleation with three-dimensional crystal growth. Finally, the formation of spherulites was obtained, which was clearly observed as reported. The two-dimensional growth could be more or less explained as the formation and growth of the lamellae. Compared with our results, the value of $n = 2.6$, through a rough handling by one linear process, suggested an ambiguous physical meaning, approximately interpreted to mean that the crystal growth was carried out between two and three dimensions.

Nonisothermal Crystallization Kinetic Analysis by the Liu–Mo Equation

The Liu–Mo equation is a method adopted to give a satisfactory analysis of the nonisothermal crystallization kinetics for semicrystalline polymers.[15,16] The good linearity of the plots for the entire process verified the advantage of the equation. According to the relationship of t and T expressed in eq. (1), for the same crystallization system, at t (or T), by the combination of the Avrami equation [eq. (2)] and the Ozawa equation, the Liu–Mo equation should be as follows:

$$\log[-\ln(1 - X_t)] = \log[K(T)] - m\log\Phi \tag{3}$$

So, the right side of the equation is equal, and eq. (3) becomes

$$\log k + n\log t = \log[K(T)] - m\log\Phi \tag{4}$$

that can be further rewritten as

$$\log\Phi = \log F(T) - a\log t \tag{5}$$

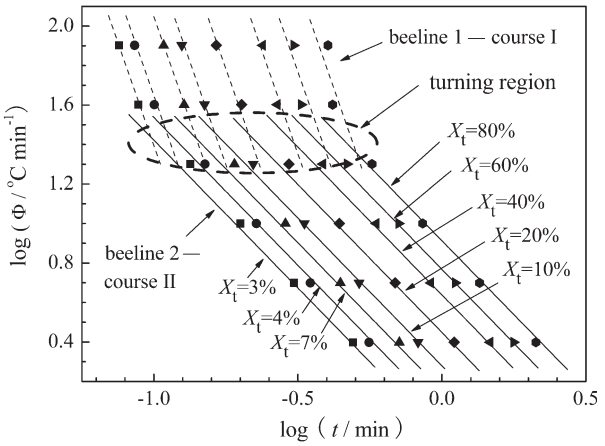

Figure 6. log ϕ versus log t for the nonisothermal crystallization of PBT.

where $F(T) = [K(T)/k]^{1/m}$ and $a = n/m$. At a given X_t, the plot of log Φ versus log t gives one straight line with $F(T)$ as the intercept and a as the slope, if available. Here $K(T)$ is the cooling function, and m is the kinetic constant related to the nucleation and crystal growth dimension mechanism of the nonisothermal crystallization, which is similar to n. $K(T)$ is a parameter related to the Φ's, and it is used to describe the nonisothermal crystallization kinetics, which have to be chosen at a unit crystallization time when the measured system amounts to a certain degree of crystallinity:

$$X_t = \frac{X_c(T)}{X_c(T_\infty)} = \int_{T_0}^{T} \frac{dH_c(T)}{dT}\,dT \Big/ \int_{T_0}^{T_\infty} \frac{dH_c(T)}{dT}\,dT \tag{6}$$

where $X_c(T)$ and $X_c(T_\infty)$ are the crystallinities at T and at complete crystallization, respectively, T_∞ represents the end temperature of crystallization, and $dH_c(T)/dT$ is the heat flow rate at T.

Generally, from eq. (5), log Φ ~ log t should be a linear relationship. The plot of log Φ versus log t for the nonisothermal crystallization of PBT, obtained from Figures 2 and 3, is shown in Figure 6. Roughly speaking, the plot of log Φ versus log t at all degrees of relative crystallinity inferred a cursory linear relationship, and the resulting average slope was $a = 1.8$.

In fact, as shown in Figure 6, the plot of log Φ versus log t was not a straight line. The resulting data plots for each X_t after careful observation indicated that there were also two processes similar to those shown in Figure 5. Because Φ, T, and t have a one-to-one relationship, the physical meaning of two turning points in the process should be very clear. The region described by beeline 1, which was in a shorter timescale, represented the beginning of the period for the nonisothermal crystallization process, and the region described by beeline 2 inferred the nonisothermal crystallization process, which was relatively long. Corresponding to each of the two beelines at the same X_t, there was a point of intersection, that is, a turning point, and all of the turning points linked together formed a turning region. From Figure 6, according to the transition region, Φ suggested a value of 30°C/min.

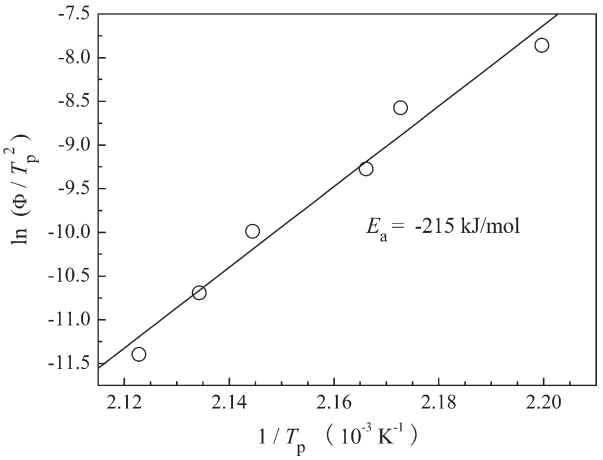

Figure 7. Kissinger plots for estimating the energy of the nonisothermal crystallization of PBT.

By analyzing the time corresponding to the transition region in Figure 6, we found the range of the transition time from course I to course II to be the same as in Figure 5, approximately in the range of 8–40 s. For nonisothermal crystallization processes under different Φ's, it was in this time range that the growth of two-dimensional lamellae changed to the three-dimensional formation of spherulites. According to the fitting ranges of each course shown in Figure 5, we found that in course I, X_t was about 1–15% and that in course II, X_t was about 15–90%. From the results obtained so far, it seemed that for each different Φ's, X_t was about 1–15% for the growth of lamellae, whereas X_t increased over 15% represented the three-dimensional growth of spherulites. The transition region corresponding to the X_t range in Figures 5 was consistent with Figure 6, as both methods had significant overlaps in the range of crystallization transition time (t), which was 8–40 s in all six cooling experiments.

From the previous discussion, we reached the conclusion that not only could the Avrami equation and Liu–Mo equation be used to describe the nonisothermal crystallization process of PBT at the same time but also both of the equations could reflect the internal connections of the two courses in the primary crystallization of the nonisothermal crystallization of PBT.

The difference between using the Liu–Mo method to analyze courses I and II in the nonisothermal primary crystallization of PBT was the changes in a and $F(T)$ of each beeline; this indicated a two-stage process. The slope of beeline 1 was larger than that of beeline 2; this suggested that there was a changeover in the primary crystallization process from course I to course II. As Figure 6 shows, the value of a was larger than 1; this indicated that n was always larger than m and suggested that significant secondary crystallization growth accompanied primary crystallization during the nonisothermal crystallization of PBT. A larger $F(T)$ suggested a faster Φ to achieve a certain X_t at a certain t. What is more, spherulite impingement also had an effect on the value of a in the nonisothermal crystallization.

E_a of the Nonisothermal Crystallization

With T_p, which is the peak temperature of the exotherm, into account, the changes with Φ, of the nonisothermal crystallization E_a were estimated with the Kissinger equation, which can be written as follows:[27]

$$d\ln(\Phi/T_p^2)/d(1/T_p) = -E_a/R \tag{7}$$

where R is the universal gas constant. From T_p, as shown in Figure 1, and the corresponding Φ, a typical plot of $\ln(\Phi/T_p^2)$ versus $1/T_p$ is presented in Figure 7. The average E_a obtained for PBT was −215 kJ/mol, as obtained from the slope of the line.

As in the practical nonisothermal crystallization process of polymers, E_a generally changed with X_t. The Kissinger equation given for E_a calculation does not take into account this factor, and the Kissinger E_a thus obtained could only be an average of the entire process. In view of the intrinsic links among E_a, Φ, the crystallization temperature, and X_t, the FWO equation was also applied to obtain E_a by the kinetic parameters. This equation is often used to calculate different E_a's at every different X_t. The FWO equation is of the form[28]

$$\log\Phi = \log[AE_a/RG(X_t)] - 2.315 - 0.4567(E_a/RT) \tag{8}$$

where A is the pre-exponential factor. $G(X_t)$ is the integral equation for nonisothermal crystallization kinetics, and its expression is

$$G(X_t) = \int_0^{X_t} dX_t/f(X_t) = (A/\Phi)\int_{T_0}^{T} \exp[-E_a/(RT)]dT \tag{9}$$

$G(X_t)$ is a constant value at different Φ's, $f(X_t)$ is a function of X_t. For the same X_t, log Φ ~ $1/T$ has a linear approximation, so for each X_t value, E_a can be calculated according to eq. (8) by the slope of the fitting of linear log Φ ~ $1/T$.

The plot of log Φ versus $1/T$ for the nonisothermal crystallization process of PBT is presented in Figure 8. Figure 8 shows the value of X_t from 1 to 95%, which basically covers the primary crystallization and the secondary crystallization of the entire nonisothermal crystallization process. The nonlinearity in the

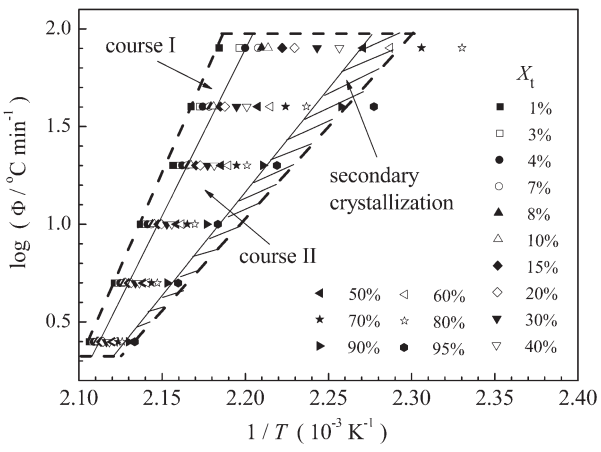

Figure 8. log ϕ versus $1/T$ for the nonisothermal crystallization of PBT.

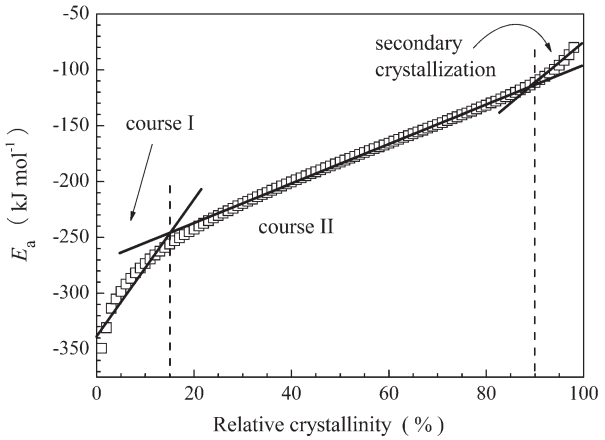

Figure 9. Relationship between E_a and X_t for the nonisothermal crystallization of PBT.

high-crystallinity area probably referred to this secondary crystallization. Figure 8 shows the schematic diagram of log Φ versus $1/T$. Each E_a could be calculated from a given X_t. The slope of each linear relationship between log Φ and $1/T$ at a given X_t decreased with increasing X_t.

According to the FWO equation, the relationship between E_a and X_t of PBT during the nonisothermal crystallization is shown in Figure 9. The figure indicates that in the entire nonisothermal crystallization process, when X_t increased, E_a decreased. E_a of the initial stage of crystallization was about 350 kJ/mol; this was higher than the following processes, whereas E_a of the late stage of crystallization decreased significantly and was eventually only 100 kJ/mol.

Figure 9 shows that E_a declined with increasing X_t, but on closer inspection, the declining rate was different. The curve of $E_a \sim X_t$ in Figure 9 could be divided into three intervals. In each interval, E_a and X_t are in an approximately linear relationship. The slope of straight line indicates varying rate of E_a with changing the relative crystallinity.

Figure 9 shows that the two intersection points of the three lines gave X_t value of about 15 and 90%. The first two intervals (1–15%) and (15–90%) were consistent with the two courses in the primary crystallization, as shown in Figure 6. Moreover, the X_t range (>90%) could be seen as secondary crystallization. Therefore, this result may then serve as a guideline for different E_a values at different courses in the nonisothermal crystallization of PBT. That is, as calculated in Figure 9, the FWO E_a's for course I, course II, and secondary crystallization were −320, −210, and −100 kJ/mol, respectively. The average of those three E_a values, −210 kJ/mol, was approximately equal to −215 kJ/mol, the E_a obtained by the Kissinger equation.

From the previous discussion, the conclusion could be reached that courses I and II indicated the lamellae and spherulites growth processes, respectively. Accordingly to the relationship $E_a \sim X_t$, as shown in Figure 9, the experimental results show that the crystal growth of lamellae in the initial stage of nonisothermal crystallization required a higher E_a. When entering the stage of the growth of spherulites, the E_a required was less than that for the growth of lamellae. At the final stage of the growth of spherulites, E_a was even lower. E_a at secondary crystallization declined gradually, along with the spherulite impingement; this was primarily because of the formation of thinner, infilling lamellae.

However, nucleation could have played a role in crystal growth, and the rate of nucleus formation depends not only on the interfacial area but also on the temperature. We are continuing to do more in-depth research and to look for more new proofs.

CONCLUSIONS

The nonisothermal crystallization behavior of PBT at six different Φ's was investigated by DSC. The crystallization rate increased with increasing Φ. The data were analyzed with the Avrami and Liu–Mo equations. The nonisothermal crystallization kinetic parameters obtained demonstrated a heterogeneous nucleation mechanism, and the primary crystallization of the nonisothermal crystallization of PBT was composed of two courses: course I for the two-dimensional process of the formation of lamellae, with a corresponding X_t of less than 15% and course II for the three-dimensional spherulite growth process, with a corresponding X_t from 15 to 90%. When X_t was greater than 90%, secondary crystallization began. In the Liu–Mo equation, the two beelines suggested that there was a changeover in the primary crystallization process from course I to course II, indicating a two-stage process.

The average E_a obtained with the Kissinger equation for the nonisothermal crystallization process of PBT was found to be −215 kJ/mol. According to the FWO equation, the E_a values for course I, course II, and secondary crystallization were calculated as −320, −210, and −100 kJ/mol, respectively.

ACKNOWLEDGMENTS

Financial support from the National Natural Science Foundation of China (No. 20974108) is acknowledged.

REFERENCES

1. Mencik, Z. *J. Polym. Sci. Polym. Phys.* **1975,** *13*, 2173.
2. Desborough, I. J.; Hall, I. H. *Polymer* **1977,** *18*, 825.
3. Nitzsche, S. A.; Wang, Y. K.; Hsu, S. L. *Macromolecules* **1992,** *25*, 2397.
4. Stein, R. S.; Misra, A. *J. Polym. Sci. Polym. Phys.* **1980,** *18*, 327.
5. Hsiao, B. S.; Wang, Z. G.; Yeh, F. J.; Gao, Y.; Sheth, K. C. *Polymer* **1999,** *40*, 3515.
6. Manabe, N.; Yokota, Y.; Minami, H.; Uegomori, Y.; Komoto, T. *J. Electron. Microsc.* **2002,** *51*, 11.
7. Di Lorenzo, M. L.; Silvestre, C. *Prog. Polym. Sci.* **1999,** *24*, 917.
8. Piorkowska, E.; Galeski, A.; Haudin, J. M. *Prog. Polym. Sci.* **2006,** *31*, 549.
9. Lehmann, B.; Karger-Kocsis, J. *J. Therm. Anal. Calorim.* **2009,** *95*, 221.

10. Kim, K. H.; Isayev, A. I.; Kwon, K. *J. Appl. Polym. Sci.* **2006,** *102*, 2847.
11. Ozawa, T. *Polymer* **1971,** *12*, 150.
12. Ziabicki, A. *Colloid Polym. Sci.* **1974,** *252*, 207.
13. Jeziorny, A. *Polymer* **1978,** *19*, 1142.
14. Gupta, A. K.; Purwar, S. N. *J. Appl. Polym. Sci.* **1984,** *29*, 1595.
15. Liu, T. X.; Mo, Z. S.; Wang, S. G.; Zhang, H. F. *Polym. Eng. Sci.* **1997,** *37*, 568.
16. Liu, T. X.; Mo, Z. S.; Zhang, H. F. *J. Appl. Polym. Sci.* **1998,** *67*, 815.
17. Huang, J. W. *J. Polym. Sci. Polym. Phys.* **2008,** *46*, 564.
18. Yao, X. Y.; Tian, X. Y.; Zheng, K.; Zhang, X.; Zheng, J.; Wang, R. X.; Liu, C.; Li, Y.; Cui, P. *J. Macromol. Sci. Phys.* **2009,** *48*, 537.
19. Al-Mulla, A.; Mathew, J.; Yeh, S. K.; Gupta, R. *Compos. A* **2008,** *39*, 204.
20. Bai, H. Y.; Zhang, Y.; Zhang, Y. X.; Zhang, X. F.; Zhou, W. *J. Appl. Polym. Sci.* **2006,** *101*, 1295.
21. Kalkar, A. K.; Deshpande, A. A. *Polym. Eng. Sci.* **2001,** *41*, 1597.
22. Wu, D. F.; Wu, L.; Yu, G. C.; Xu, B.; Zhang, M. *Polym. Eng. Sci.* **2008,** *48*, 1057.
23. Wunderlich, B. Macromolecular Physics: Crystal Nucleation, Growth, Annealing; Academic: New York, **1976.**
24. Gilbert, M.; Hybart, F. *J. Polymer* **1972,** *13*, 327.
25. Marrs, W.; Peters, R. H.; Still, R. H. *J. Appl. Polym. Sci.* **1979,** *23*, 1077.
26. Righetti, M. C.; Munari, A. *Macromol. Chem. Phys.* **1997,** *198*, 363.
27. Kissinger, H. E. *J. Res. Natl. Bur. Stand.* **1956,** *57*, 217.
28. Flynn, J. H.; Wall, L. A. *J. Polym. Sci. Polym. Lett.* **1966,** *4*, 323.